Hydrogermylation initiated by trialkylborohydrides: a living anionic mechanism

Maciej Zaranek*[a,b], Mateusz Nowicki[b], Piotr Andruszak[b], Marcin Hoffmann[b], and Piotr Pawluć[a,b]

a) Centre for Advanced Technologies, Adam Mickiewicz University, Uniwersytetu Poznańskiego st. 10, 61-614 Poznań, Poland
b) Faculty of Chemistry, Adam Mickiewicz University, Uniwersytetu Poznańskiego st. 8, 61-614 Poznań, Poland
** m.zaranek@amu.edu.pl*

Abstract. Sodium trialkylborohydrides were found to be selective catalysts for the hydrogermylation of aromatic alkenes. Addition of phenylgermane and diphenylgermane in the presence of 10 mol% of NaHB(*sec*-Bu)$_3$ proceeded in a highly selective manner to give – in contrast to the analogous hydrosilylation process – *β*-germylated products. The nature of this process was explained with the aid of DFT calculations and it was proposed that the mechanism proceeds via a trisubstituted germanide anion whose attack on the terminal vinyl carbon is the source of selectivity.

Hydrogermylation of terminal alkenes and alkynes (Scheme 1) is a powerful transformation for catalytic synthesis of organogermanes.

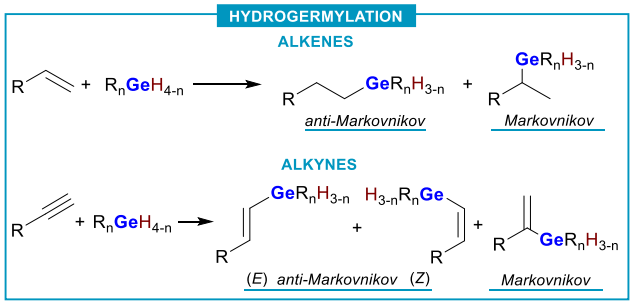

Scheme 1. Hydrogermylation

The addition of hydrogermanes across multiple carbon – carbon bonds typically relies on the activation of the Ge-H bond by transition metal complexes (mainly Pd, Ru, Rh, and Pt)[1] or radical initiators such as Et_3B/O_2 and AIBN.[2]

Recently, a new generation of catalysts based on earth- abundant first- row transition metal carbonyl complexes of Fe,[3] Mn[4], and Co[5] have also attracted considerable attention. Moreover, hydrogermylation of alkynes[6] as well as transfer hydrogermylation of alkenes[7] have been successfully achieved using transition metal-free, boron-containing catalyst: $B(C_6F_5)_3$. However, to the best of our knowledge there is no report on the use of commercially available alkali metal trialkylborohydrides in this process.

The position of germanium between silicon and tin in group 14 of the periodic table causes organogermanium compounds to exhibit properties similar to those of organosilicon and organotin compounds, however, the synthetic chemistry of this element is still in its infancy, and therefore, organogermanes have not received significant attention.[8] On the other hand, organogermanes have found use as essential cross-coupling partners in selective carbon−carbon bond formation reactions to circumvent the limitations of traditional organometallic reagents. Recent progress in the application of organogermanes has been outlined in the work of Schoenebeck and Fricke, who have shown that organogermanium compounds possess unique and complementary reactivity in relation to that of other

organometallic coupling agents, paving the way for their further interesting applications in organic synthesis.[9]

We have already reported that $NaHBEt_3$ can be used as a catalyst for Markovnikov selective hydrosilylation of aromatic alkenes[10,11] and dehydrogenative silylation of terminal alkynes.[12] $NaHBEt_3$ has also been demonstrated by Thomas and coworkers to catalyze hydroboration of phenylacetylene with pinacolborane to give (*E*)-styryl boronic ester.[13] Given the growing interest in application of organogermanes in organic synthesis and the mechanistic similarity of the hydrosilylation and hydroboration to already known occurrences of hydrogermylation, we decided to study the reactivity of alkali metal triethylborohydrides in the presence of aromatic alkenes and primary and secondary germanes to examine the impact of these commonly used reductants on the course of the hydrogermylation process.

Driven by previous successful experiments in hydrosilylation, we initialized the research on hydrogermylation by screening the catalytic activity of different trialkylborohydrides in a reaction of diphenylgermane with styrene. Also as previously, toluene has been used as a solvent and reactions were carried out for 20 hours at 100 °C. The first experiments unfolded unexpectedly, producing diphenyl (2-phenylethyl) germane exclusively, a product of opposite regioselectivity compared to hydrosilylation (Scheme 2).

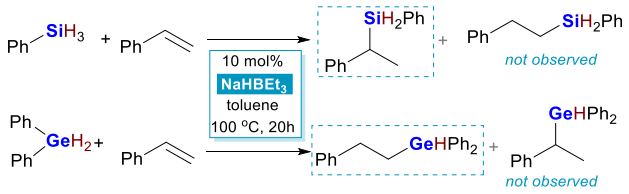

Scheme 2. Opposite selectivity of hydrosilylation and hydrogermylation under the same conditions.

Out of several commercially available trialkylborohydrides, i.e. $LiHBEt_3$, $NaHBEt_3$, $NaH(sec\text{-}Bu)_3$, and $KHBEt_3$, it was the third one that exhibited the best selectivity and reactivity. As observed also in other research, lithium triethylborohydride turned out to promote unwanted side reactions, whereas its potassium congener led to formation of heavier products of consequent hydrogermylation (*higher-order products*). Decreasing the amount of sodium tri(*sec*-butyl)borohydride resulted in a decrease in conversion of diphenylgermane, and thus a loading of 10% has been maintained in the subsequent experiments.

Several conjugated aromatic alkenes were hydrogermylated by phenyl- and diphenylgermane, as shown in the Chart 1. It is worth noting that tri(*n*-butyl)germane was inactive under the conditions used in this research. The isolation of adducts of phenylgermane turned out to be challenging. The instability of $PhGeRH_2$ towards hydrolysis precluded chromatographic purification methods, as most of these products could not be retrieved from the chromatography column, even when silanised silica was used as a stationary phase. These compounds were identified only by gas chromatography coupled with mass spectrometry (GC-MS). It was, however, possible to purify six exemplary compounds, whose analysis further confirmed that hydrogermylation aided by tri(*sec*-butyl)borohydride yields products with anti-Markovnikov selectivity. Among those was the product of hydrogermylation of 2-vinylnaphthalene with phenylgermane, **6**. To better explain these findings, we turned to the theoretical simulation of possible reaction pathways by means of DFT methods.[‡]

It appeared natural to begin the theoretical investigation with an approach described in our previous research.[11] After initial calculations (for details, see SI), the conclusion was drawn that regardless of the final regioselectivity, the reaction was initiated by a nucleophilic attack of a $NaHBMe_3$ hydride anion on the terminal carbon atom of styrene (Chart 2, **M** superscript), which is preferred over the attack at the benzylic carbon (**aM** superscript). The observations for phenylgermane are almost identical as for phenylsilane.

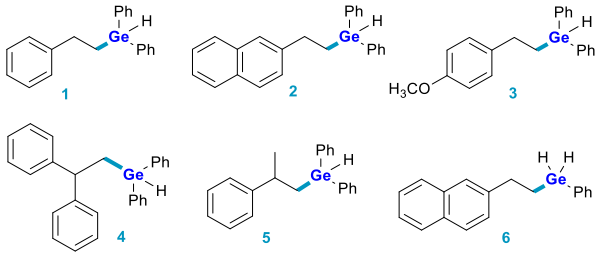

Chart 1. Products of NaHB(*s*-Bu)$_3$ assisted hydrogermylation.

the methodology applied in this study. Despite its coherency, this mechanism cannot be applied to hydrogermylation since its occurrence would result in the formation of Markovnikov products.

Instead, the reaction pathway that should be discussed (Chart 3), proceeds after sodium dihydro(phenyl)germanide **VII** is formed. This species attacks a styrene molecule at the terminal carbon atom and produces a carbanion (**IX-XI**). The latter is again a secondary, resonance-stabilized one. This time, however, the germanium atom is at the anti-Markovnikov position. The final product **XV** is released after this carbanion abstracts a hydrogen cation from phenylgermane (**XII-XIV**) and regenerates sodium dihydro(phenyl)germanide for the next cycle.

The analysis of Chart 3 delivers a precise explanation for the anti-Markovnikov mode of reaction between phenylgermane and styrene. Starting from **V**, a barrier of only ca. 11.5 kcal/mol (**VI**) has to be overcome to generate NaPhGeH$_2$ (**VII**). This step can be seen as essentially irreversible as the reverse reaction would require ca. 30 kcal/mol. The cycle itself includes two transition states: a relative 16.5 kcal/mol one of styrene activation **X**, and a 13 kcal/mol one of sodium dihydro(phenyl)germanide regeneration **XIII**. the former is much lower than activation of styrene by NaHBMe$_3$ (23 kcal/mol) and provides a convincing explanation for the anti-Markovnikov mode of reaction. Gibbs free energy profiles display similar features for diphenylgermane (for details, see SI).

The mode of initial generation of the essential sodium dihydro(phenyl)germanide has found further support in an experiment showing that increase in the amount of NaHB(*sec*-Bu)$_3$ resulted in proportional increase of the amount of ethylbenzene formed.

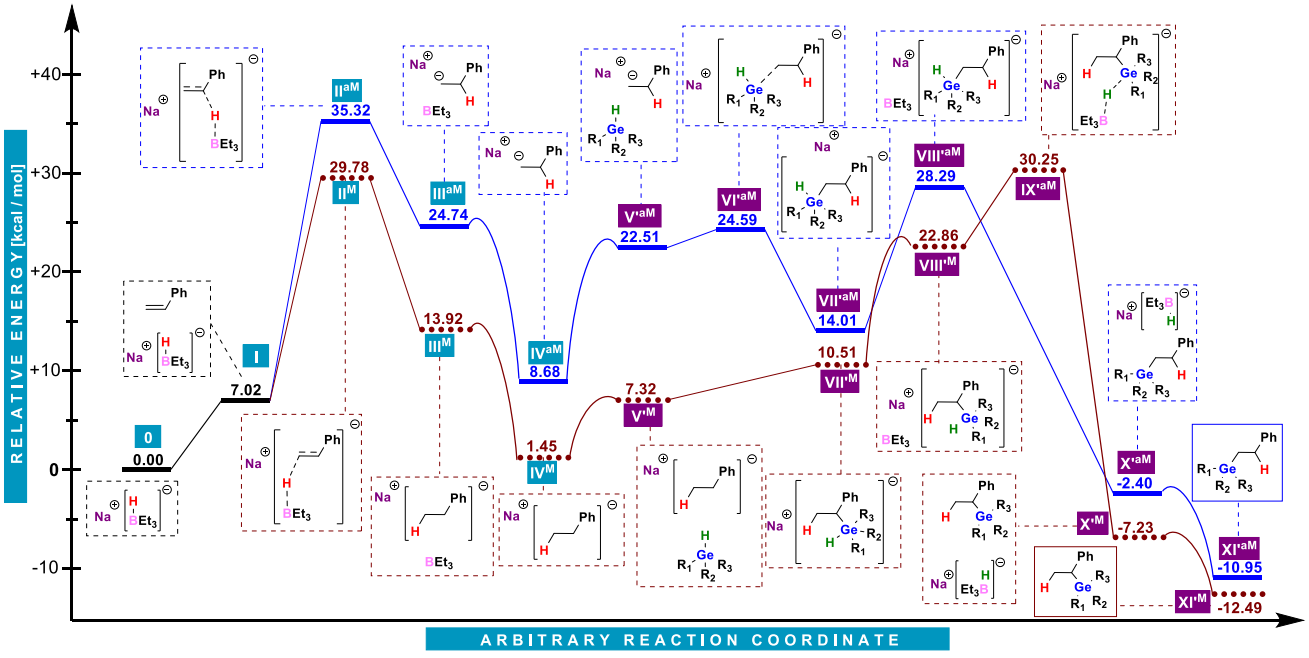

Chart 2. Energy profiles calculated for possible hydrogermylation pathways analogous to already published hydrosilylation mechanism.

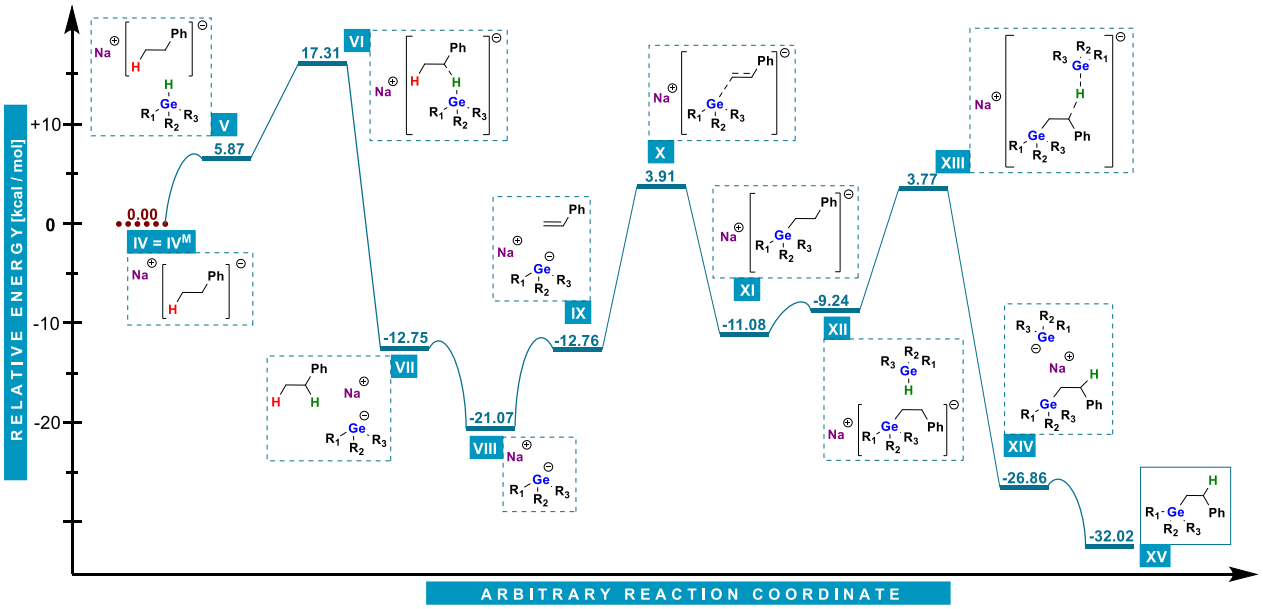

Chart 3. DFT energy calculation of the most possible pathway of anti-Markovnikov hydrogermylation in the presence of alkali metal trialkylborohydrides.

Altogether, we have demonstrated that sodium tri(sec-butyl)borohydride is a good initiator of anti-Markovnikov selective hydrogermylation of conjugated aromatic alkenes. It is not, however, a catalyst of this process, since the reaction proceeds via a germanide anion, which is regenerated in the last step, and no borohydride moiety is further needed. This can result in the conclusion that hydrogermylation in this reaction system can be seen as a 'living' process.

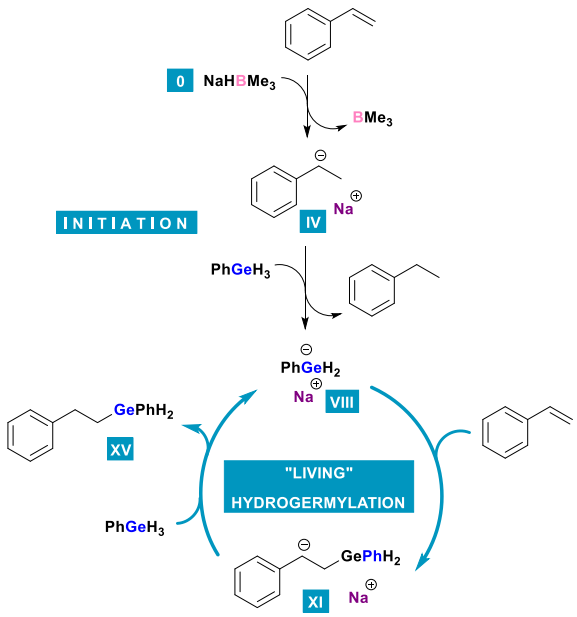

Scheme 3. Proposed mechanism of “living” anionic hydrogermylation of styrenes.

Acknowledgements

This research was financially supported by the National Science Centre (Poland), grant № UMO-2016/23/B/ST5/0017. Computations were carried out using the PL-Grid infrastructure. MZ gratefully acknowledges financial support of the Foundation for Polish Science, grant № START 96.2020. MN gratefully acknowledges grant no. POWR.03.02.00-00-I020/17 co-financed by the European Union through the European Social Fund under the Operational Program Knowledge Education Development. Submitted in partial satisfaction of the requirements for the PhD degree (MN).

Notes and references

‡ DFT calculations. For details, see SI.

Initial structures of reactants were generated with usual values of bond lengths and valence angles[14] and were followed by full geometry optimization toward potential energy minima. In these and subsequent computations, M06-2X/6-31++G(d,p)/LANL2DZdp level of theory[15,16,25,17–24] was employed (LANL2DZdp basis set for Si and Ge atoms and 6-31++G(d,p) for other atoms). Based on our previous research, triethylborane was substituted with trimethylborane in order to reduce computational complexity at a negligible change in relative energies of respective structures. To identify possible reaction pathways, we conducted relaxed potential energy scans while controlling 1 or 2 interatomic distances. Whenever a scan did not result in a new stationary point, the path was discarded; otherwise, synchronous transit-guided quasi-Newton approach (**QST3**)[26] was used to determine the geometry of the respective transition state (TS), followed by a pseudo **IRC**[27] calculation to confirm or generate potential energy minima that are connected by a given TS. For all stationary points identified throughout the research, force constants and the resulting vibrational modes (**freq** calculations) were computed. Each of these calculations was carried out for molecules dissolved in toluene within the polarizable continuum model (PCM).[28] For thermochemical calculations, the standard pressure p = 1.00000 atm and the temperature T = 373.150 K were applied. The Gaussian 16 program package was used for all quantum-chemical computations.[29] Basis Set Exchange resource was used to optimize the level of theory employed.[30]

1 A. P. Dobbs and F. K. I. Chio, in *Comprehensive Organic Synthesis II, 2nd ed.*, eds. P. Knochel and G. A. Molander, Elsevier, 2014, pp. 964–998.
2 H. Yorimitsu and K. Oshima, *Inorg. Chem. Commun.*, 2005, **8**, 131–142.
3 M. Itazaki, M. Kamitani and H. Nakazawa, *Chem. Commun.*, 2011, **47**, 7854.
4 H. Liang, Y.-X. Ji, R.-H. Wang, Z.-H. Zhang and B. Zhang, *Org. Lett.*, 2019, **21**, 2750–2754.
5 M. R. Radzhabov and N. P. Mankad, *Org. Lett.*, 2021, **23**, 3221–3226.
6 T. S. and and V. Gevorgyan*, *Org. Lett.*, 2005, **7**, 5191–5194.
7 S. Keess and M. Oestreich, *Org. Lett.*, 2017, **19**, 1898–1901.
8 T. Akiyama, in *Main Group Metals in Organic Synthesis*, eds. H. Yamamoto and K. Oshima, Wiley-VCH, Weinheim, 2004, pp. 593–619.
9 C. Fricke and F. Schoenebeck, *Acc. Chem. Res.*, 2020, **53**, 2715–2725.
10 M. Zaranek, S. Witomska, V. Patroniak and P. Pawluć, *Chem. Commun.*, 2017, **53**, 5404–5407.
11 M. Nowicki, M. Zaranek, P. Pawluć and M. Hoffmann, *Catal. Sci. Technol.*, 2020, **10**, 1066–1072.
12 M. Skrodzki, S. Witomska and P. Pawluć, *Dalt. Trans.*, 2018, **47**, 5948–5951.
13 N. W. J. Ang, C. S. Buettner, S. Docherty, A. Bismuto, J. R. Carney, J. H. Docherty, M. J. Cowley and S. P. Thomas, *Synthesis (Stuttg).*, 2017, **50**, 803–808.
14 A. K. Rappe, C. J. Casewit, K. S. Colwell, W. A. Goddard and W. M. Skiff, *J. Am. Chem. Soc.*, 1992, **114**, 10024–10035.
15 Y. Zhao and D. G. Truhlar, *Theor. Chem. Acc.*, 2008, **120**, 215–241.
16 T. Clark, J. Chandrasekhar, G. W. Spitznagel and P. V. R. Schleyer, *J. Comput. Chem.*, 1983, **4**, 294–301.
17 J. D. Dill and J. A. Pople, *J. Chem. Phys.*, 1975, **62**, 2921–2923.
18 R. Ditchfield, W. J. Hehre and J. A. Pople, *J. Chem. Phys.*, 1971, **54**, 724–728.
19 M. M. Francl, W. J. Pietro, W. J. Hehre, J. S. Binkley, M. S. Gordon, D. J. DeFrees and J. A. Pople, *J. Chem. Phys.*, 1982, **77**, 3654–3665.
20 M. S. Gordon, J. S. Binkley, J. A. Pople, W. J. Pietro and W. J. Hehre, *J. Am. Chem. Soc.*, 1982, **104**, 2797–2803.

21 P. C. Hariharan and J. A. Pople, *Theor. Chim. Acta*, 1973, **28**, 213–222.
22 W. J. Hehre, R. Ditchfield and J. A. Pople, *J. Chem. Phys.*, 1972, **56**, 2257–2261.
23 G. W. Spitznagel, T. Clark, P. von Ragué Schleyer and W. J. Hehre, *J. Comput. Chem.*, 1987, **8**, 1109–1116.
24 C. E. Check, T. O. Faust, J. M. Bailey, B. J. Wright, T. M. Gilbert and L. S. Sunderlin, *J. Phys. Chem. A*, 2001, **105**, 8111–8116.
25 W. R. Wadt and P. J. Hay, *J. Chem. Phys.*, 1985, **82**, 284–298.
26 C. Peng and H. Bernhard Schlegel, *Isr. J. Chem.*, 1993, **33**, 449–454.
27 K. Fukui, *Acc. Chem. Res.*, 1981, **14**, 363–368.
28 S. Miertuš, E. Scrocco and J. Tomasi, *Chem. Phys.*, 1981, **55**, 117–129.
29 J. Frisch, G. W. Trucks, H. B. Schlegel, G. E. Scuseria, M. A. Robb, J. R. Cheeseman, G. Scalmani, V. Barone, B. Mennucci, G. A. Petersson, H. Nakatsuji, M. Caricato, X. Li, H. P. Hratchian, A. F. Izmaylov, J. Bloino, G. Zheng, J. L. Sonnenberg, M. Hada, M. Ehara, K. Toyota, R. Fukuda, J. Hasegawa, M. Ishida, T. Nakajima, Y. Honda, O. Kitao, H. Nakai, T. Vreven, J. A. J. Montgomery, J. E. Peralta, F. Ogliaro, M. Bearpark, J. J. Heyd, E. Brothers, K. N. Kudin, V. N. Staroverov, T. Keith, R. Kobayashi, J. Normand, K. Raghavachari, A. Rendell, J. C. Burant, S. S. Iyengar, J. Tomasi, M. Cossi, N. Rega, J. M. Millam, M. Klene, J. E. Knox, J. B. Cross, V. Bakken, C. Adamo, J. Jaramillo, R. Gomperts, R. E. Stratmann, O. Yazyev, A. J. Austin, R. Cammi, C. Pomelii, J. W. Ochterski, R. L. Martin, K. Morokuma, V. G. Zakrzewski, G. A. Voth, P. Salvador, J. J. Dannenberg, S. Dapprich, A. D. Daniels, V. Ortiz, J. Cioslowski and D. J. Fox, 2013.
30 B. P. Pritchard, D. Altarawy, B. Didier, T. D. Gibson and T. L. Windus, *J. Chem. Inf. Model.*, 2019, **59**, 4814–4820.